J. Plasma Phys. (2016), *vol.* 82, 535820401
doi:10.1017/S0022377816000647

Orientation of the X-line in asymmetric magnetic reconnection

N. Aunai[1],†, M. Hesse[2], B. Lavraud[3], J. Dargent[1] and R. Smets[1]

[1]Laboratoire de Physique des Plasmas, CNRS, Ecole Polytechnique, Université Pierre et Marie Curie, Université Paris-Sud, Observatoire de Paris, France

[2]NASA Goddard Space Flight Center, Heliophysics Division, Greenbelt, MD, USA

[3]Institut de Recherche en Astrophysique et Planétologie, CNRS, Université Paul Sabatier, Toulouse, France

(Received 15 April 2016; revised 9 June 2016; accepted 14 June 2016)

Magnetic reconnection can occur in current sheets separating magnetic fields sheared by any angle and of arbitrarily different amplitudes. In such asymmetric and non-coplanar systems, it is not yet understood what the orientation of the X-line will be. Studying how this orientation is determined locally by the reconnection process is important to understand systems such as the Earth magnetopause, where reconnection occurs in regions with large differences in upstream plasma and field properties. This study aims at determining what the local X-line orientation is for different upstream magnetic shear angles in an asymmetric set-up relevant to the Earth's magnetopause. We use two-dimensional hybrid simulations and vary the simulation plane orientation with regard to the fixed magnetic field profile and search for the plane maximizing the reconnection rate. We find that the plane defined by the bisector of upstream fields maximizes the reconnection rate and this appears not to depend on the magnetic shear angle, domain size or upstream plasma and asymmetries.

1. Introduction

Magnetic reconnection is recognized as a universal way to release large amounts of magnetic energy stored within current sheets into plasma kinetic and thermal energy, as well as enabling large-scale transport through magnetic boundaries (Biskamp 2005; Birn & Priest 2007; Priest & Forbes 2007). The canonical configuration for reconnection is often depicted as a current sheet separating two sets of coplanar and oppositely directed magnetic field lines. Most reconnection models have been based on this configuration (Parker 1957; Birn *et al.* 2001). The models also often assume two-dimensionality of the problem for the sake of simplicity. These models match perhaps most closely the environments of planetary magnetotails and very fruitful comparisons between numerical models of antiparallel reconnection and *in situ* spacecraft measurements have been achieved (Paschmann 2008; Eastwood *et al.* 2010; Fuselier & Lewis 2011; Eastwood *et al.* 2013). However, tail configurations remain very special in light of the much broader set of geometrical and physical configurations reconnection can encounter in other systems. Among these, the closest are the solar corona (Aulanier *et al.* 2006), the solar wind (Phan *et al.* 2006*a*;

† Email address for correspondence: nicolas.aunai@lpp.polytechnique.fr

Gosling *et al.* 2007), the Earth's magnetopause or even at the heliopause, where the interstellar field supposedly reconnects with the heliospheric one (Swisdak *et al.* 2010). In general magnetic reconnection can occur in asymmetric current sheets, involve field lines with an arbitrary shear angle and evolve in a three-dimensional fashion (Hesse & Schindler 1988; Hesse *et al.* 2005*b*; Hesse, Forbes & Birn 2005*a*). In these cases, even basic questions such as what the local orientation of the reconnection line remain unanswered.

This simple question of orientation may have profound implications on reconnecting systems, their modelling and observation. It is expected that the reconnection rate, the dissipated magnetic energy etc. will strongly depend on which magnetic components are merging. Most analytical models have been based on the values of the reconnecting components (e.g. Swisdak *et al.* 2003; Cassak & Shay 2007), rather than on the magnetic amplitudes. The observational signatures and dynamical evolution predicted by two-dimensional numerical models will change depending on the plane that the evolution is forced to occur in. At the Earth magnetopause, where the process reconnects magnetosheath field lines draped around the Earth dipole to magnetospheric field lines, the interpretation of spacecraft measurements, almost always assumed to be obtained from quasi two-dimensional structures, will also depend on which plane one chooses to project vectors onto.

The question of the local orientation of X-lines is also related to the question of the locations where reconnection occurs. On the magnetopause surface, both *in situ* and remote observations reveal that reconnection signatures, such as accelerated particles and flows, exhibit a macroscopic pattern evolving with the variation of interplanetary magnetic field (IMF) and consistent with a macroscopic merging line on the magnetopause (e.g. Scurry, Russell & Gosling 1994; Dunlop *et al.* 2005; Phan *et al.* 2006*b*; Trattner *et al.* 2007*a*,*b*; Trenchi *et al.* 2008 and references therein). This interpretation connects the orientation problem to the location problem, the latter being the integral of the former. It is not entirely clear, though, whether the local X-line orientation is physically determined by a global process, which *a priori* imposes the location of a macroscopic X-line. Alternatively, it could result from the local and self-consistent dynamics of the reconnection process, thereby *a posteriori* determining where the macroscopic X-line is, or even be determined by a complex coupling between global and local scale processes.

In a global organization scenario, the local orientation is merely reactive, in a way that reconnection is locally oriented because of some larger-scale constraints imposed on the global properties of the magnetopause by the magnetosphere–solar wind coupling. In other words, given one point of an X-line and the associated upstream conditions, the surrounding properties of the magnetopause determine the X-line location. Early models suggested the merging line would be found only in nearly antiparallel regions (Crooker 1979) but observations (Paschmann 2008) required a generalization to include non-coplanar events as well. Other ideas were, for instance, that the reconnection line would follow regions of maximized current density (Alexeev, Sibeck & Bobrovnikov 1998) or follow a path so as to maximize the magnetic shear angle (Trattner *et al.* 2007*a*,*b*). Another idea also suggests the reconnection line may more probably be found at the location of a global magnetic separator (Siscoe *et al.* 2001; Dorelli, Bhattacharjee & Raeder 2007). The magnetic separator location in three-dimensional (3-D) global resistive magnetohydrodynamics (MHD) simulations (Komar, Fermo & Cassak 2015) was later compared to various theories for different IMF orientations. No prediction perfectly mapped the separator location.

Another way of addressing this problem is to assume, on the contrary, that the X-line orientation is entirely determined locally, i.e. that a reconnection X-line locally

https://doi.org/10.1017/S0022377816000647 Published online by Cambridge University Press

and self-consistently orients itself independently from the mesoscale or macroscale variations of physical quantities on the magnetopause. The orientation would only depend on the upstream parameters, i.e. on the physical properties of immediately adjacent regions in the magnetosphere and magnetosheath. This dynamics may very well be controlled by 3-D or 2-D mechanisms as long as it is local. This idea is appealing since magnetopause variations along the X-line are generally thought to be on a much larger scale than those in the other two directions, and also because not all points along a global line can be causally related and therefore must evolve independently for some time at least. Many ideas have been proposed to explain which direction the X-line could be aligned with, as a function of only local parameters and dynamics. An early idea was that reconnection would occur in the plane for which upstream guide fields are equal, i.e. the plane locally perpendicular to the local average magnetopause current density vector (Sonnerup 1974). This imposes strong constraints on the reconnection process since, depending on the amplitude asymmetry between the upstream fields, such a plane does not necessarily contain in-plane components that reverse sign, and therefore may forbid reconnection. Although no justification has been found as to why reconnection would be impossible in such cases, this scenario is still widely used. Indeed, most observation studies by far tacitly assume the directions of the reconnecting, out-of-plane and normal magnetic components are respectively equivalent to the directions of the $\boldsymbol{L}$, $\boldsymbol{M}$ and $\boldsymbol{N}$ eigenvectors obtained from the minimum variance analysis, e.g. (Phan *et al.* 2013). Also, most 2-D asymmetric simulations model non-coplanar reconnection by simply adding a uniform guide field (i.e. not associated with in-plane currents) to an antiparallel configuration, therefore tacitly fixing the reconnection plane, e.g. (Pritchett & Mozer 2009; Aunai *et al.* 2013*b*). Global X-line models have also been built with other rules such as that of following vectors that bisect the local upstream magnetic fields (Moore, Fok & Chandler 2002), or that are perpendicular to the plane containing antisymmetric components (Cowley 1976). Other and more recent ideas may be grouped under the same argument that reconnection will locally orient itself so that it processes magnetic flux the fastest, i.e. so that it maximizes the reconnection rate. They however differ because of the different understanding of how the rate could be maximized. It has been shown, for instance, that in non-coplanar asymmetric reconnection, in-plane diamagnetic drifts along the outflow direction could strongly alter reconnection, even preventing it from occurring. Favoured planes could therefore be those where such an effect is minimized (Swisdak *et al.* 2003). However, depending on the asymmetry of the current sheet, it may be possible that no plane shows this effect, which can therefore not be universally used to determine the X-line orientation. Another idea is that maximizing the outflow velocity (Swisdak & Drake 2007), as given by (1.1), should be close enough from maximizing the reconnection rate.

This velocity is given by:

$$v_{out} \propto B_u B_d \frac{B_u + B_d}{\rho_u B_d + \rho_d B_u}, \tag{1.1}$$

where B_u and B_d are the absolute value of the merging magnetic components and $\rho_{u,d}$ the upstream (up and down sides of the current sheet) mass densities.

A generalization was to use the Cassak & Shay (2007) scaling laws of the reconnection rate derived for asymmetric systems (1.2) or similar ones (Birn *et al.* 2010) and to find the plane that locally maximizes it (Borovsky 2013).

$$R \propto \frac{B_u B_d}{B_u + B_d} v_{out}. \tag{1.2}$$

https://doi.org/10.1017/S0022377816000647 Published online by Cambridge University Press

Both ideas were found to be in reasonable agreement with a 3-D resistive MHD simulation of asymmetric reconnection in an initially planar current sheet (Schreier *et al.* 2010). Yet another idea is to actually perform a series of 2-D simulations rotated around the direction normal to the initial current sheet, and empirically determine which one makes reconnection the fastest. Such experiment has been realized recently with fully kinetic particle-in-cell (PIC) simulations (Hesse *et al.* 2013). It was then shown, with a single magnetic and plasma initial set-up, that the variation of the maximum reconnection rate with the simulation plane is well described by the variation of the product of the in-plane upstream magnetic energy densities (1.3).

$$R_b \propto B_u^2 B_d^2. \tag{1.3}$$

The plane maximizing (1.3) is identical to the plane normal to the bisector of the upstream fields. Perhaps the strongest limitation of this study was the neglect of possible self-consistent reconnection dynamics developing in the third direction, which could change the result. This point was addressed in a subsequent study (Liu, Hesse & Kuznetsova 2015), where the same initial set-up was studied using both 2-D and 3-D fully kinetic simulations. X-lines in 3-D systems were consistently found to naturally orient along the bisector, in both the nonlinear phase of the reconnection process and the linear phase of the tearing instability. A mass ratio dependency was found, which again was consistent between 2-D and 3-D models, and suggested that even models with realistic mass ratio would align with the bisector.

On the observational side, most studies focused on the magnetopause X-line addressed this issue from a global perspective, as discussed before. Local determination of the X-line orientation have been addressed much more rarely. A possibility, again assuming quasi-2-D dynamics, is to determine for which direction of space fields and plasma properties are the most invariant, using reconstruction techniques (Teh & Sonnerup 2008; Teh *et al.* 2009). With a single measurement and a large associated uncertainty, it is however hard to say whether the data agree more with one model or another. Such an issue would need to be tackled in a statistical manner for a panel of varying shear angles, assuming that the measured upstream shear angles are similar to those relevant for the reconnection dynamics at the X-line.

This paper addresses the issue of X-line orientation as a function of local parameters and dynamics. Like previous studies (Hesse *et al.* 2013; Liu *et al.* 2015), we perform a set of 2-D simulations and rotate the simulation plane to find the orientation that maximizes the reconnection rate. Our specific goal here is to know to what extent these results depend on the domain size, the initial field and plasma asymmetries and on the magnetic shear angle. Therefore, for a similar magnetic shear angle ($\sim 90°$), we first use a different magnetic amplitude and plasma asymmetry. Then, keeping the field amplitude and plasma asymmetry unchanged, we vary the magnetic shear angle. The paper is organized as follows: the second section describes the numerical model and initial condition we use. The third section describes our methodology and the results we obtain. The fourth part is a discussion of the results and the conclusion of this paper.

2. Numerical model and initial set-up

Although previous studies have mainly used fully kinetic models to study how the local reconnection dynamics orients the X-line, the use of a PIC code (Aunai *et al.* 2013*b*) seems well suited for the present study. Hybrid models solve ion dynamics

https://doi.org/10.1017/S0022377816000647 Published online by Cambridge University Press

following the PIC algorithm, while electrons appear only via their first three fluid equations. As they do not need to resolve electron kinetic scales, hybrid models can be used advantageously for parametric studies such as this one, enabling us to use larger boxes and longer simulation times. Hybrid simulations of asymmetric magnetic reconnection have been shown to lead to results very similar to those obtained with fully kinetic models (Aunai *et al.* 2013*b*). In the model, the electron density n_e is assumed to be equal to the ion density n at all time and spatial scales, the electron momentum equation (2.1) is used to calculate the electric field, assuming negligible bulk inertia and a simple isothermal closure for their pressure P_e. An additional term of hyper-resistivity $-\nu\nabla^2\boldsymbol{j}$ is used and is known to be better at defining a proper dissipation scale than standard resistivity (Aunai *et al.* 2013*a*).

$$\boldsymbol{E} = -\boldsymbol{v}_e \times \boldsymbol{B} - \frac{1}{ne}\nabla P_e - \nu\nabla^2\boldsymbol{j}. \tag{2.1}$$

Equations and numerical values presented in this paper are normalized. The magnetic field is normalized by a typical field B_0 and the time by the proton cyclotron frequency eB_0/m_p, where e and m_p are the elementary electric charge and proton mass, respectively. The particle density is normalized by a density n_0, which characterizes the denser upstream region in the simulations presented here. Distances are normalized by the proton inertial length δ_p associated with n_0.

Using these units, all simulations described in this paper are performed in a physical domain of size (400, 80) in the (x, y) plane, using a uniform Cartesian mesh having $(n_x, n_y) = (2000, 800)$ cells. The boundary condition in the y direction is perfectly conducting for the fields and reflective for particles. The x direction is periodic. A total of approximately 500 million macroparticles is used. Previous studies using rotating reconnection planes (Hesse *et al.* 2013; Liu *et al.* 2015) were done using an upstream magnetic amplitude and density ratio of 3. We therefore use a different set-up. In our case, the density is given by (2.2), where $n_1 = 1$ and $n_2 = 0.25$

$$n(y) = n_1 + \frac{n_2 - n_1}{2}(1 + \tanh(y_0)). \tag{2.2}$$

The magnetic field amplitude and components are given by (2.3)–(2.5), where $B_1 = 0.5$ and $B_2 = 1$. The ion temperature initially balances the total pressure, assuming $\beta_1 = n_1 T_1/B_1^2 = 7$ and a constant electron temperature $T_e = 0.2$. Magnetic reconnection is triggered with a centred perturbation of amplitude $\delta B \approx 0.1$. The current sheet is positioned at $y = y_0 = 40$. The simulations are evolved until $T = 400$ with a time step $\Delta t = 0.001$. The hyper-resistive coefficient ν is set to 10^{-4}.

$$B(y) = B_1 + 0.5(B_2 - B_1)(1 + \tanh(y - y_0)) \tag{2.3}$$

$$B_x(y) = B\cos(\alpha(y)) \tag{2.4}$$

$$B_z(y) = B\sin(\alpha(y)). \tag{2.5}$$

The angle α represents the smooth rotation of the magnetic field from one side of the current sheet to the other and its profile is given by (2.6), where $\alpha_2 - \alpha_1$ is the magnetic shear angle ψ. The angles α_1 and α_2 represent the angles between the magnetic field and the x axis on each side of the current sheet.

$$\alpha(y) = \alpha_1 + \frac{\alpha_2 - \alpha_1}{2}(1 + \tanh(y - y_0)). \tag{2.6}$$

https://doi.org/10.1017/S0022377816000647 Published online by Cambridge University Press

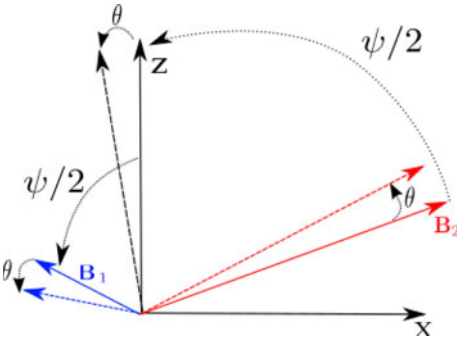

FIGURE 1. The simulations are performed in the (x, y) plane. The reconnecting component are aligned with the x axis, the z axis is therefore in the out of plane direction, and, in our 2-D models, also represents the direction of the X-line. The initial upstream magnetic field vectors are represented by the solid red ($\boldsymbol{B_2}$) and solid blue ($\boldsymbol{B_1}$) vectors. Equations (2.3)–(2.5) describe the smooth transition along y between $\boldsymbol{B_1}$ and $\boldsymbol{B_2}$. The magnetic field is initially oriented so that the z axis bisects $\boldsymbol{B_1}$ and $\boldsymbol{B_2}$. The angle θ rotates the profiles of $\boldsymbol{B_1}$ and $\boldsymbol{B_2}$ around the y axis. The coloured dashed arrows represent the rotated magnetic field. The dashed black arrow represents the bisector of the rotated upstream field vectors.

Run	ψ	θ
R_1	90	0
R_2	90	−15
R_3	90	15
R_4	90	25
R_5	130	0
R_6	130	−25
R_7	130	30

TABLE 1. Table detailing the runs we have performed, with their magnetic shear angle ψ and their orientation θ with respect to the bisection of upstream magnetic field vectors.

It is important to note that, contrary to usual set-ups, we vary the magnetic shear angle but keep the plasma and its magnetization unchanged. This is important since other effects such as particle magnetization are known to affect the reconnection process (Hesse *et al.* 2013). We run four simulations (called runs R_1, R_2, R_3 and R_4) for which the magnetic shear is $\psi = 90°$, which is similar to the one used by Hesse *et al.* (2013), Liu *et al.* (2015), therefore enabling us to isolate the role of plasma and field amplitude asymmetries. Another series of 3 runs, called R_5, R_6 and R_7, then keep the plasma and field amplitude asymmetry identical but change the magnetic shear angle to $\psi = 130°$. Each simulation uses an initial magnetic set-up rotated by an angle θ with respect to the direction bisecting $\boldsymbol{B_1}$ and $\boldsymbol{B_2}$. Figure 1 represents the magnetic configuration and shows the important angles. Table 1 summarizes the values of the angles we use. Figures 2 and 3 represent the initial values of the upstream merging components on both sides of the current sheet as a function of the simulation plane orientation θ, for runs with $\psi = 90°$ and $\psi = 130°$, respectively.

https://doi.org/10.1017/S0022377816000647 Published online by Cambridge University Press

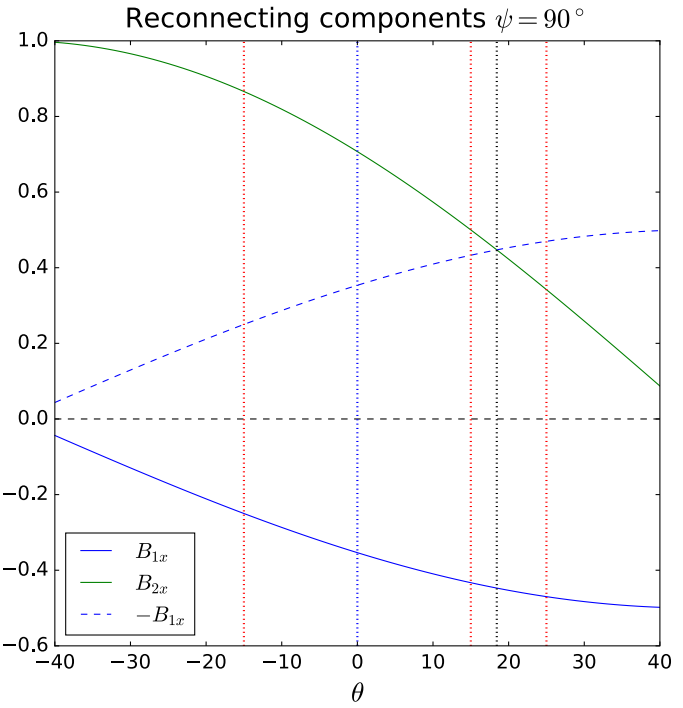

FIGURE 2. Reconnecting components as a function of the orientation angle θ for $\psi = 90°$. The blue and green solid lines represent the initial values taken by the merging components in the upstream regions. The dashed blue line represents $-B_{x1}$ to ease the comparison with B_{x2}. The dotted blue vertical line represents the simulation performed at $\theta = 0$, the two dotted red ones represent the simulations $\theta = \pm 15$ and $\theta = 25$. The dotted black vertical line represents the orientation giving identical upstream guide fields, which for $\psi = 90°$ is also the orientation of antisymmetric merging components.

We see in those figures that rotations towards negative values of θ make the merging components more asymmetric while positive values of θ make them more symmetric than at the bisector orientation.

3. Results

Our goal is to determine empirically the plane orientation, which results in the fastest reconnection process, and then compare the results to theories previously used in this context as potentially good candidates for predicting the orientation maximizing the rate. We chose the following theories: (i) the bisection prediction given by (1.3), because it was found to have a good agreement in previous studies (Hesse *et al.* 2013; Liu *et al.* 2015) for a different initial set-up; (ii) the Cassak & Shay (2007) rate scaling law given by (1.2), because its purpose is to give an estimate of the asymmetric reconnection rate as a function of upstream parameters. We will also compare the orientation of the maximum rate with the one making the upstream guide field uniform (Sonnerup 1974), widely used in observational studies, and with the one where merging components are equal (Cowley 1976). We essentially need, for each simulation, to select one characteristic rate value, report it on a plot versus the plane orientation θ and check which orientation leads to a maximum

https://doi.org/10.1017/S0022377816000647 Published online by Cambridge University Press

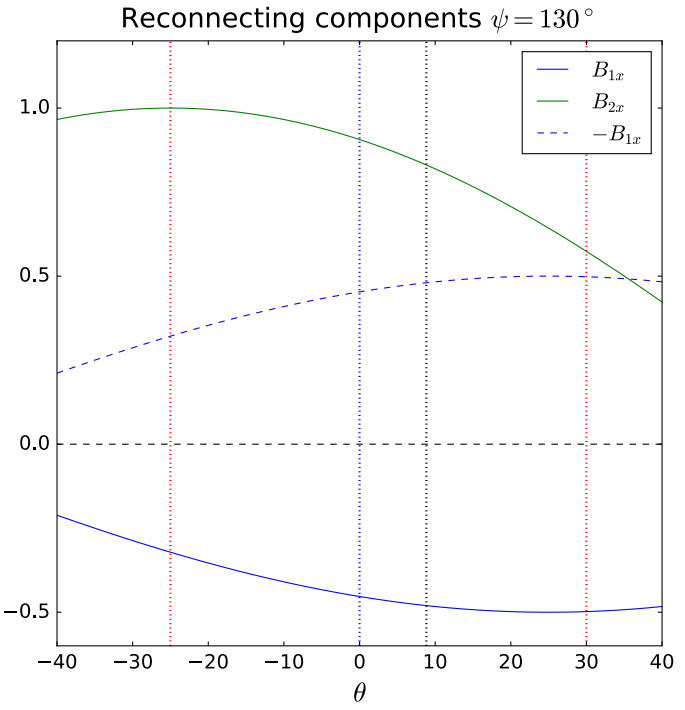

FIGURE 3. Same format as figure 2 for runs having $\psi = 130°$, red vertical dashed lines mark $\theta = 30°$ and $\theta = -25°$.

reconnection rate and whether the observed rate variation agrees with one of the above theories or follows a different trend. There are several ways one can do this. Previous research (Hesse *et al.* 2013; Liu *et al.* 2015) used the maximum reconnection rate as a characteristic value, having in mind that, for a given orientation, it gives an upper limit to what the rate can be. However, due to small domains, one cannot be absolutely sure the observed peak rate is not an artefact of the limitations of the simulation domain. Here, for consistency with these studies, we also use this method, but the use of much larger domains eliminates the influence of domain boundaries at the time of maximum rate. Also, because the theories we compare our results to are not focused on describing the rate at its peak value or at any other specific time, we want to consider more data and therefore also evaluate the average reconnection rate for each simulation. This answers the question of what plane orientation reconnects the most flux in a given time. The time averaging period being also arbitrary, we use three different ones and check to what extent it changes the results. Figures 4 and 5 show the reconnection rate for all simulations as a function of time. They show the value for the peak reconnection rate we have selected, and the time periods that have been used to compute averaged reconnection rates. The plots already show that the simulation aligned with the bisector has the fastest rate of all. Simulations for $\psi = 90°$ oriented at $\theta = \pm 15°$ have similar maximum rates but different time evolutions. Similar behaviour is observed for simulations with $\psi = 130°$, negative θ leads to a longer time taken in reaching the peak rate than for positive θ. This difference must be related to the merging components becoming more asymmetric as θ becomes negative and more symmetric as θ becomes positive, as reported earlier on figures 2 and 3.

https://doi.org/10.1017/S0022377816000647 Published online by Cambridge University Press

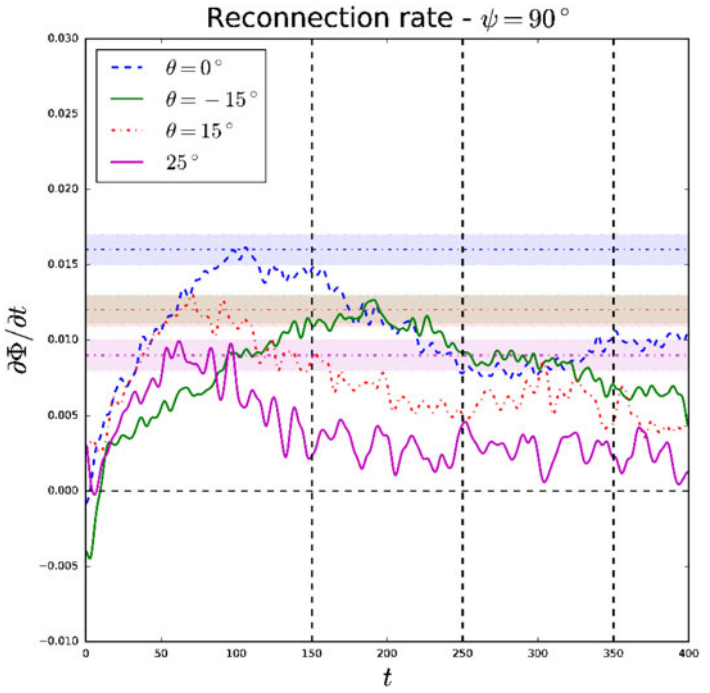

FIGURE 4. Reconnection rate as a function of time for runs $R_{1..4}$ ($\psi = 90°$). The horizontal dashed lines mark the value of the maximum rate for each simulation, the rectangular area of the same colour represents the associated uncertainty in selecting the maximum, which changes slightly with the smoothing kernel used on the raw rate data. The red and green maxima are identical, making the rectangle brownish. The black vertical dashed lines represent the upper time limit to the time averaging periods used to compute the averaged reconnection rates, the lower time limit being $t = 0$.

Figure 6(*d*) shows the maximum rate as a function of the simulation orientation θ. Equations (1.2) and (1.3), normalized by the maximum value of the data points, are also shown. One can see the two theories predict essentially the same rate variation for negative θ, but are clearly different for positive values of θ. The data points seem in a better agreement with the bisection model than with the other ones. In particular, data indicate the reconnection rate is small for the orientation that makes upstream guide fields equal. For $\psi = 90°$, this direction also lead to antisymmetric merging components, which is therefore not the fastest reconnection plane either. Even when considering the averaged reconnection rate, visible in (*a–c*), the conclusion stays the same. The plane oriented by the bisector reconnects the most flux in all three time averaging periods, and the other orientations are aligned almost perfectly with the bisection model. Results from runs $R_{1..4}$ therefore agree well with previous studies, suggesting that the different initial field amplitude and plasma asymmetries do not change these conclusions.

Now keeping the field amplitude and plasma initial profiles identical, runs $R_{5..7}$ use a different magnetic shear angle $\psi = 130°$. Figure 7 has the same format as figure 6 but now shows data for runs $R_{5..7}$. One can see that again that the plane oriented with the bisector of the upstream field has the highest maximum rate (*d*) and reconnects the most flux in all time averaging periods (*a–c*). Other runs have been performed at large

https://doi.org/10.1017/S0022377816000647 Published online by Cambridge University Press

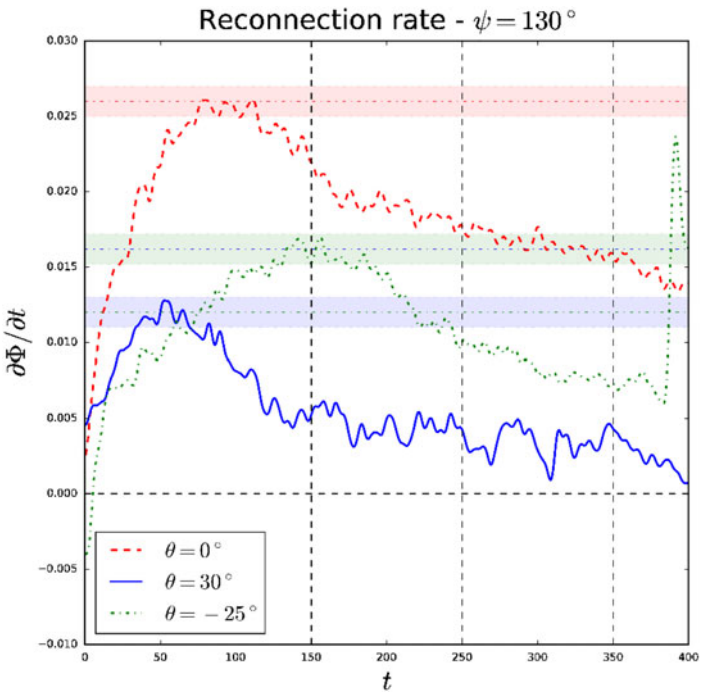

FIGURE 5. Reconnection rate as a function of time for runs $R_{5..7}$ ($\psi = 130°$). See figure 4 for the format description.

angular distance from the bisector because the larger width of the theoretical curves makes them less distinguishable for small angles. At these orientations (including $\theta = 30°$ which is close to antisymmetric merging components, see figure 3), the maximum rate and the average rates are significantly lower than for the bisector orientation, and close to the bisection model prediction. (*a–c*) Show the average reconnection rates for each simulation for different time averaging windows. Overall, the trend followed by the data points are again in better agreement with the bisection model.

4. Discussion

In this work, we aimed at determining how the reconnection X-line self-consistently orients itself as a function of local upstream parameters only. Assuming 2-D variations, and following results of Liu *et al.* (2015), we postulate that the orientation of the X-line is associated with the plane where reconnection processes the most magnetic flux, i.e. where the reconnection rate is maximized. Hybrid simulations were performed where reconnection occurs within an asymmetric current sheet for two different magnetic shears, 90° and 130°. The simulations support the idea that the reconnection rate is maximized when the process occurs in the plane defined by the bisector of upstream magnetic field vectors. Its variation with the system orientation seems to follow the variation of the in-plane magnetic energy (Hesse *et al.* 2013) better than the Cassak & Shay (2007) rate scaling law. A reason for this is perhaps that the latter has been derived considering antiparallel magnetic fields, and may therefore not be adequate to describe reconnection rates in non-coplanar systems. Orientations for which upstream merging components are equal (Cowley 1976), or

https://doi.org/10.1017/S0022377816000647 Published online by Cambridge University Press

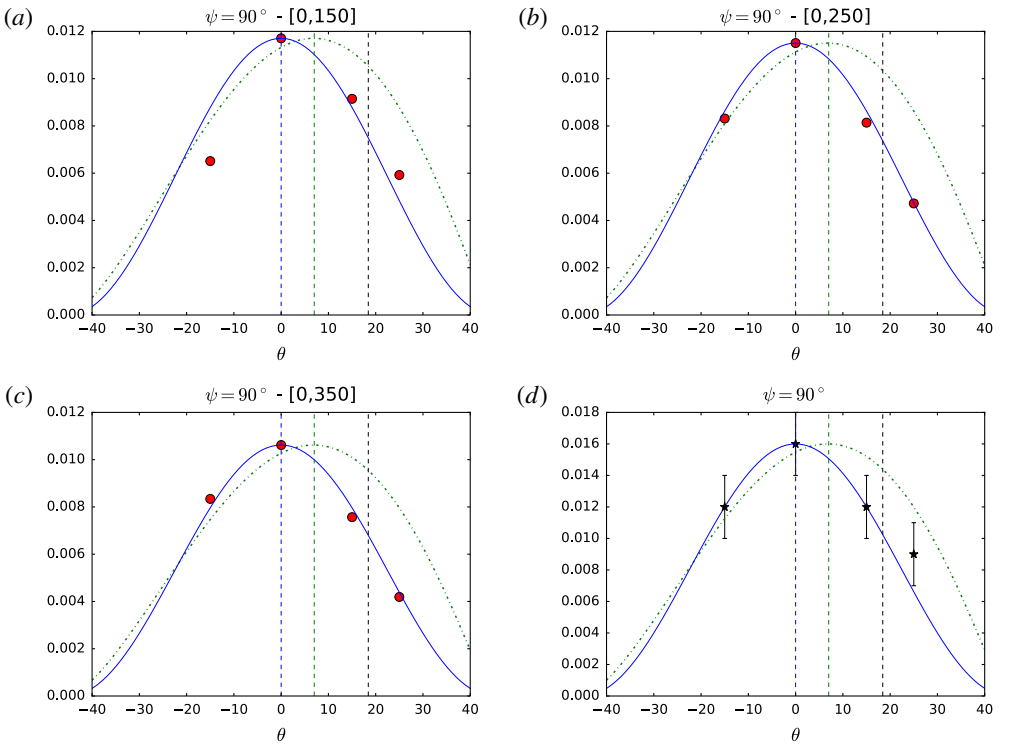

FIGURE 6. Results for runs $R_{1..4}$ with $\psi = 90°$. (*a–c*) Show as red dots the reconnection rate averaged during different time intervals specified in the title of each plot, as a function of the simulation plane orientation θ. (*d*) Shows the maximum reconnection rates with their associated uncertainty. For (*a–d*), the solid blue and dash-dot green curves represent equations (1.2) and (1.3), respectively, normalized by the maximum value of the data points.

for which the guide field is identical (Sonnerup 1974) do not result in the fastest reconnection rate. These results do not depend on the shear angle between upstream magnetic fields. Furthermore, simulations $R_{1..4}$ have a similar shear angle but different magnetic and plasma asymmetries than previous works (Hesse *et al.* 2013; Liu *et al.* 2015). Finding again the bisector orientation, we can therefore conclude the problem seems not to depend on these parameters either.

It is of interest to note that our results were obtained from a hybrid model, which, by design, does not include electron kinetic physics. The fact that our results match those of 2-D and 3-D fully kinetic models seems to suggest that ion kinetic effects may be important players in setting X-line orientations. This idea is appealing since, due to their much larger mass, it seems likely that either thermal or bulk ion kinetic effects have to be involved in determining the overall reconnection dynamics. In theory, hybrid models also include electron diamagnetic drifts, which are known to possibly alter the reconnection dynamics (Swisdak *et al.* 2003) whenever the X-line drifts faster than the Alfvén speed based on upstream characteristics. In our runs, the X-line slowly move in the positive x direction, which is opposed to the electron diamagnetic drift velocity based on the positive B_z and density gradient $\partial_y n < 0$. For other initial parameters, and assuming they remain relevant once reconnection is

https://doi.org/10.1017/S0022377816000647 Published online by Cambridge University Press

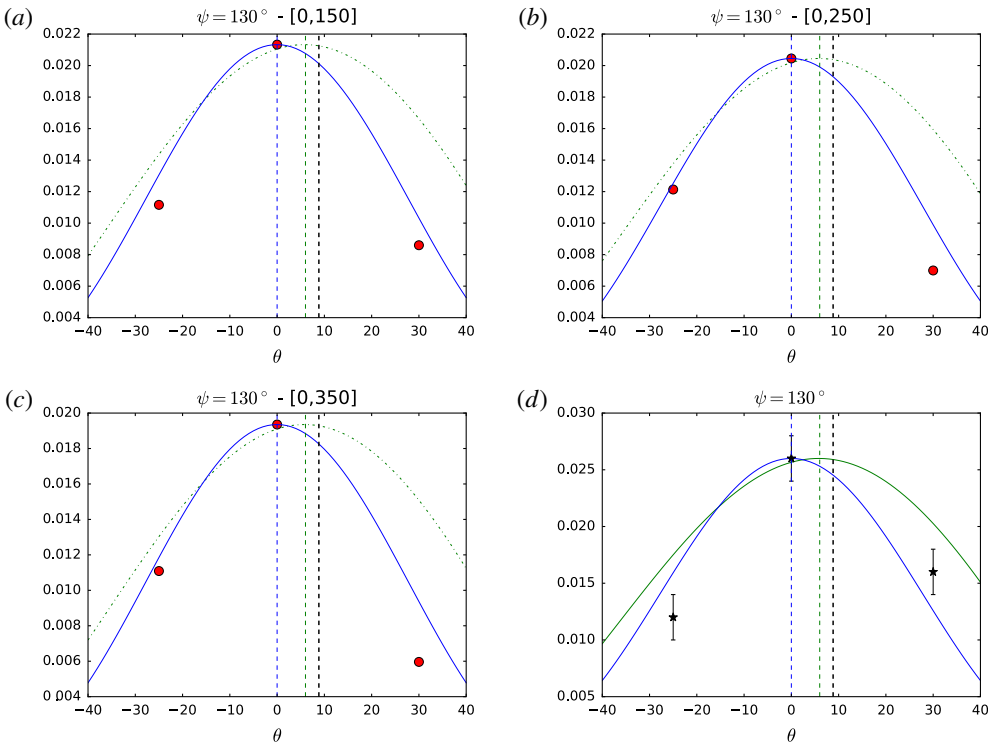

FIGURE 7. Results for runs $R_{5..7}$ with $\psi = 130°$. See figure 6 for the format.

ongoing, diamagnetic effects may change the conclusion of this study regarding the fastest reconnection plane. Also, the electron pressure is generally not very realistic in a hybrid model. It remains unclear to what extent electron kinetic physics, leading to more complex pressure tensors, is important for this effect. More research is necessary to evaluate the differences between hybrid and fully kinetic magnetopause reconnection modelling, one way is, for example, to account for a more realistic electron closure in hybrid codes (Le *et al.* 2016).

In the context of the magnetopause, our simulations and those of (Hesse *et al.* 2013; Liu *et al.* 2015) can be seen as local and independent, reconnecting magnetopause patches having different plasma and field asymmetries and different shear angles between the upstream magnetic field vectors. Together, they indicate that reconnection may locally orient itself to evolve in the fastest reconnection plane, which is also the one defined by the bisector of upstream field vectors. Knowing one point where reconnection occurs on the magnetopause, and assuming everything is determined locally, one may follow the bisector direction and draw a macroscopic reconnection line. If all the points along this line represent the local fastest reconnection planes, they would however not necessarily be the locations of maximized reconnection rate on the magnetopause surface, or the location of the most probable onset. This connects to the problems of where reconnection starts at the magnetopause, whether it spreads and where and how different reconnection events interact with each other to give a global pattern.

In our simulations, the X-line is well defined. Other recent simulations in 3-D also show well defined X-lines (Liu *et al.* 2015) However, in some situations, which

https://doi.org/10.1017/S0022377816000647 Published online by Cambridge University Press

remain to be clarified, reconnection can dynamically produce flux ropes, i.e. many X-lines for which the orientation may differ, although upstream plasma and field characteristics are homogeneous (Daughton *et al.* 2011). In such cases, defining a unique X-line orientation may be difficult. A possibility for 3-D fragmented current sheets is to define the orientation as the one of a dominant X-line, for which the integral of $E_{\parallel}$ is the largest through all non-ideal regions of the system (Wyper & Hesse 2015). Knowing whether such a stable dominant X-line generally arise is an important unresolved question.

Progress on the connection between local X-line orientation and global magnetopause X-lines requires efforts to fill the gap between the local effects discussed here and the global scales, by progressively adding microphysics in global simulations and larger-scale variations in kinetic models.

Acknowledgements

The authors would like to thank the two anonymous reviewers for their comments. The numerical simulations presented in this study have been performed at IDRIS on supercomputer ADA in the project x2016047231. This work is part of the ANR project MONANR: ANR-13-PDOC-0027.

REFERENCES

ALEXEEV, I. I., SIBECK, D. G. & BOBROVNIKOV, S. Y. 1998 Concerning the location of magnetopause merging as a function of the magnetopause current strength. *J. Geophys. Res.* **103** (A), 6675–6684.

AULANIER, G., PARIAT, E., DÉMOULIN, P. & DEVORE, C. R. 2006 Slip-running reconnection in quasi-separatrix layers. *Solar Phys.* **238** (2), 347–376.

AUNAI, N., HESSE, M., BLACK, C., EVANS, R. & KUZNETSOVA, M. 2013*a* Influence of the dissipation mechanism on collisionless magnetic reconnection in symmetric and asymmetric current layers. *Phys. Plasmas* **20** (4), 042901.

AUNAI, N., HESSE, M., ZENITANI, S., KUZNETSOVA, M., BLACK, C., EVANS, R. & SMETS, R. 2013*b* Comparison between hybrid and fully kinetic models of asymmetric magnetic reconnection: coplanar and guide field configurations. *Phys. Plasmas* **20** (2), 2902,1–10.

BIRN, J., BOROVSKY, J. E., HESSE, M. & SCHINDLER, K. 2010 Scaling of asymmetric reconnection in compressible plasmas. *Phys. Plasmas* **17** (5), 2108.

BIRN, J., DRAKE, J. F., SHAY, M. A., ROGERS, B. N., DENTON, R. E., HESSE, M., KUZNETSOVA, M., MA, Z. W., BHATTACHARJEE, A., OTTO, A. *et al.* 2001 Geospace environmental modeling (GEM) magnetic reconnection challenge. *J. Geophys. Res.* **106** (A), 3715–3720.

BIRN, J. & PRIEST, E. R. 2007 *Reconnection of Magnetic Fields*. Cambridge University Press.

BISKAMP, D. 2005 *Magnetic Reconnection in Plasmas*. Cambridge University Press.

BOROVSKY, J. E. 2013 Physical improvements to the solar wind reconnection control function for the Earth's magnetosphere. *J. Geophys. Res. Space* **118** (5), 2113–2121.

CASSAK, P. A. & SHAY, M. A. 2007 Scaling of asymmetric magnetic reconnection: general theory and collisional simulations. *Phys. Plasmas* **14** (1), 2114.

COWLEY, S. W. H. 1976 Comments on the merging of nonantiparallel magnetic fields. *J. Geophys. Res.* **81**, 3455–3458.

CROOKER, N. U. 1979 Dayside merging and cusp geometry. *J. Geophys. Res.* **84** (A3), 951–959.

DAUGHTON, W., ROYTERSHTEYN, V., KARIMABADI, H., YIN, L., ALBRIGHT, B. J., BERGEN, B. & BOWERS, K. J. 2011 Role of electron physics in the development of turbulent magnetic reconnection in collisionless plasmas. *Nat. Phys.* **7** (7), 539–542.

DORELLI, J. C., BHATTACHARJEE, A. & RAEDER, J. 2007 Separator reconnection at Earth's dayside magnetopause under generic northward interplanetary magnetic field conditions. *J. Geophys. Res.* **112** (A), 02202.

DUNLOP, M. W., TAYLOR, M. G. G. T., DAVIES, J. A., OWEN, C. J., PITOUT, F., FAZAKERLEY, A. N., PU, Z., LAAKSO, H., BOGDANOVA, Y. V., ZONG, Q.-G. *et al.* 2005 Coordinated cluster/double star observations of dayside reconnection signatures. *Ann. Geophys.* **23** (8), 2867–2875.

EASTWOOD, J. P., PHAN, T. D., DRAKE, J. F., SHAY, M. A., BORG, A. L., LAVRAUD, B. & TAYLOR, M. G. G. T. 2013 Energy partition in magnetic reconnection in Earth's magnetotail. *Phys. Rev. Lett.* **110** (2), 225001.

EASTWOOD, J. P., PHAN, T. D., ØIEROSET, M. & SHAY, M. A. 2010 Average properties of the magnetic reconnection ion diffusion region in the Earth's magnetotail: the 2001–2005 cluster observations and comparison with simulations. *J. Geophys. Res.* **115** (A), 08215.

FUSELIER, S. A. & LEWIS, W. S. 2011 Properties of near-Earth magnetic reconnection from in-situ observations. *Space Sci. Rev.* **160** (1), 95–121.

GOSLING, J. T., ERIKSSON, S., BLUSH, L. M., PHAN, T. D., LUHMANN, J. G., MCCOMAS, D. J., SKOUG, R. M., ACUÑA, M. H., RUSSELL, C. T. & SIMUNAC, K. D. 2007 Five spacecraft observations of oppositely directed exhaust jets from a magnetic reconnection X-line extending 4.26×106 km in the solar wind at 1 AU. *Geophys. Res. Lett.* **34** (2), 20108.

HESSE, M., AUNAI, N., ZENITANI, S., KUZNETSOVA, M. & BIRN, J. 2013 Aspects of collisionless magnetic reconnection in asymmetric systems. *Phys. Plasmas* **20** (6), 1210.

HESSE, M., FORBES, T. G. & BIRN, J. 2005*a* On the relation between reconnected magnetic flux and parallel electric fields in the solar corona. *Astrophys. J.* **631** (2), 1227–1238.

HESSE, M., KUZNETSOVA, M., SCHINDLER, K. & BIRN, J. 2005*b* Three-dimensional modeling of electron quasiviscous dissipation in guide-field magnetic reconnection. *Phys. Plasmas* **12** (10), 100704.

HESSE, M. & SCHINDLER, K. 1988 A theoretical foundation of general magnetic reconnection. *J. Geophys. Res.* **93**, 5559–5567.

KOMAR, C. M., FERMO, R. L. & CASSAK, P. A. 2015 Comparative analysis of dayside magnetic reconnection models in global magnetosphere simulations. *J. Geophys. Res. Space* **120** (1), 276–294.

LE, A., DAUGHTON, W., KARIMABADI, H. & EGEDAL, J. 2016 Hybrid simulations of magnetic reconnection with kinetic ions and fluid electron pressure anisotropy. *Phys. Plasmas* **23** (3), 032114.

LIU, Y.-H., HESSE, M. & KUZNETSOVA, M. 2015 Orientation of X lines in asymmetric magnetic reconnection—mass ratio dependency. *J. Geophys. Res. Space* **120** (9), 7331–7341.

MOORE, T. E., FOK, M. C. & CHANDLER, M. O. 2002 The dayside reconnection X line. *J. Geophys. Res. Space* **107** (A), 1332.

PARKER, E. N. 1957 Sweet's mechanism for merging magnetic fields in conducting fluids. *J. Geophys. Res.* **62**, 509–520.

PASCHMANN, G. 2008 Recent in-situ observations of magnetic reconnection in near-Earth space. *Geophys. Res. Lett.* **35** (1), 19109.

PHAN, T. D., GOSLING, J. T., DAVIS, M. S., SKOUG, R. M., ØIEROSET, M., LIN, R. P., LEPPING, R. P., MCCOMAS, D. J., SMITH, C. W., RÈME, H. *et al.* 2006*a* A magnetic reconnection X-line extending more than 390 Earth radii in the solar wind. *Nature* **439** (7), 175–178.

PHAN, T. D., HASEGAWA, H., FUJIMOTO, M., ØIEROSET, M., MUKAI, T., LIN, R. P. & PATERSON, W. 2006*b* Simultaneous geotail and wind observations of reconnection at the subsolar and tail flank magnetopause. *Geophys. Res. Lett.* **33** (9), 09104.

PHAN, T. D., SHAY, M. A., GOSLING, J. T., FUJIMOTO, M., DRAKE, J. F., PASCHMANN, G., ØIEROSET, M., EASTWOOD, J. P. & ANGELOPOULOS, V. 2013 Electron bulk heating in magnetic reconnection at Earth's magnetopause: dependence on the inflow Alfvén speed and magnetic shear. *Geophys. Res. Lett.* **40** (1), 4475–4480.

PRIEST, E. & FORBES, T. 2007 *Magnetic Reconnection*. Cambridge University Press.

PRITCHETT, P. L. & MOZER, F. S. 2009 Asymmetric magnetic reconnection in the presence of a guide field. *J. Geophys. Res.* **114** (A), 11210.

SCHREIER, R., SWISDAK, M., DRAKE, J. F. & CASSAK, P. A. 2010 Three-dimensional simulations of the orientation and structure of reconnection X-lines. *Phys. Plasmas* **17** (1), 0704.

SCURRY, L., RUSSELL, C. T. & GOSLING, J. T. 1994 A statistical study of accelerated flow events at the dayside magnetopause. *J. Geophys. Res.* **99**, 14815.

SISCOE, G. L., ERICKSON, G. M., SONNERUP, B. U. O., MAYNARD, N. C., SIEBERT, K. D., WEIMER, D. R. & WHITE, W. W. 2001 Global role of E parallel in magnetopause reconnection: an explicit demonstration. *J. Geophys. Res.* **106** (A), 13015–13022.

SONNERUP, B. U. O. 1974 Magnetopause reconnection rate. *J. Geophys. Res.* **79** (1), 1546.

SWISDAK, M. & DRAKE, J. F. 2007 Orientation of the reconnection X-line. *Geophys. Res. Lett.* **34** (1), 11106.

SWISDAK, M., OPHER, M., DRAKE, J. F. & ALOUANI BIBI, F. 2010 The vector direction of the interstellar magnetic field outside the heliosphere. *Astrophys. J.* **710** (2), 1769–1775.

SWISDAK, M., ROGERS, B. N., DRAKE, J. F. & SHAY, M. A. 2003 Diamagnetic suppression of component magnetic reconnection at the magnetopause. *J. Geophys. Res. Space* **108** (A), 1218.

TEH, W.-L. & SONNERUP, B. U. O. 2008 First results from ideal 2-D MHD reconstruction: magnetopause reconnection event seen by cluster. *Ann. Geophys.* **26** (9), 2673–2684.

TEH, W.-L., SONNERUP, B. U. O., HU, Q. & FARRUGIA, C. J. 2009 Reconstruction of a large-scale reconnection exhaust structure in the solar wind. *Ann. Geophys.* **27** (2), 807–822.

TRATTNER, K. J., MULCOCK, J. S., PETRINEC, S. M. & FUSELIER, S. A. 2007*a* Location of the reconnection line at the magnetopause during southward IMF conditions. *Geophys. Res. Lett.* **34** (3), 03108.

TRATTNER, K. J., MULCOCK, J. S., PETRINEC, S. M. & FUSELIER, S. A. 2007*b* Probing the boundary between antiparallel and component reconnection during southward interplanetary magnetic field conditions. *J. Geophys. Res.* **112** (A), 08210.

TRENCHI, L., MARCUCCI, M. F., PALLOCCHIA, G., CONSOLINI, G., BAVASSANO CATTANEO, M. B., DI LELLIS, A. M., RÈME, H., KISTLER, L., CARR, C. M. & CAO, J.-B. 2008 Occurrence of reconnection jets at the dayside magnetopause: double star observations. *J. Geophys. Res.* **113** (A).

WYPER, P. F. & HESSE, M. 2015 Quantifying three dimensional reconnection in fragmented current layers. *Phys. Plasmas* **22** (4), 042117.

Nicolas Aunai

Nicolas Aunai did his PhD in 2011 at the Laboratory of Plasma Physics (LPP) at the Ecole Polytechnique, near Paris in France, under supervision of Gerard Belmont and Roch Smets. His PhD thesis focused on the ion kinetic mechanisms underlying the fluid description of collisionless magnetic reconnection, which he studied via kinetic hybrid simulations and spacecraft observations and theory – a work for which he received the 'René Pellat award' of the plasma division of the French Physical Society in 2012. He later joined the NASA Goddard Space Flight Center, USA, to work with Michael Hesse's team. During his time in the USA, Nicolas Aunai's research mainly targeted magnetopause asymmetric reconnection, focusing on comparisons between fully and hybrid kinetic modelling of this process. In 2013, he joined the Institute for Resarch in Astrophysics and Planetology (IRAP), Toulouse, France, where he started a project joining IRAP, LPP and NASA researchers on modelling and observations of magnetopause reconnection, at the dawn of the launch of the NASA Magnetospheric MultiStale mission. In 2014 Nicolas was recruited as a permanent researcher at LPP/CNRS, where he continues his research on magnetic reconnection, focusing on its multiscale aspect, relationships between fluid/kinetic formalisms, the role of multiple particle populations and the development of new techniques for analysing *in situ* spacecraft measurements.

https://doi.org/10.1017/S0022377816000647 Published online by Cambridge University Press